Published OnlineFirst May 20, 2013; DOI: 10.1158/0008-5472.CAN-13-0529

Cancer Research

# Neuropilin-2 Promotes Extravasation and Metastasis by Interacting with Endothelial α5 Integrin

Ying Cao, Luke H. Hoeppner, Steven Bach, et al.

*Cancer Res* 2013;73:4579-4590. Published OnlineFirst May 20, 2013.

Published OnlineFirst May 20, 2013; DOI: 10.1158/0008-5472.CAN-13-0529

*Tumor and Stem Cell Biology*

Cancer Research

# Neuropilin-2 Promotes Extravasation and Metastasis by Interacting with Endothelial α5 Integrin

Ying Cao[1], Luke H. Hoeppner[1], Steven Bach[2], Guangqi E[1], Yan Guo[2], Enfeng Wang[1], Jianmin Wu[3], Mark J. Cowley[3], David K. Chang[3,4,5], Nicola Waddell[6], Sean M. Grimmond[6], Andrew V. Biankin[3,4,5], Roger J. Daly[3], Xiaohui Zhang[2], and Debabrata Mukhopadhyay[1]

## Abstract

Metastasis, the leading cause of cancer death, requires tumor cell intravasation, migration through the bloodstream, arrest within capillaries, and extravasation to invade distant tissues. Few mechanistic details have been reported thus far regarding the extravasation process or re-entry of circulating tumor cells at metastatic sites. Here, we show that neuropilin-2 (NRP-2), a multifunctional nonkinase receptor for semaphorins, vascular endothelial growth factor (VEGF), and other growth factors, expressed on cancer cells interacts with α5 integrin on endothelial cells to mediate vascular extravasation and metastasis in zebrafish and murine xenograft models of clear cell renal cell carcinoma (RCC) and pancreatic adenocarcinoma. In tissue from patients with RCC, NRP-2 expression is positively correlated with tumor grade and is highest in metastatic tumors. In a prospectively acquired cohort of patients with pancreatic cancer, high NRP-2 expression cosegregated with poor prognosis. Through biochemical approaches as well as Atomic Force Microscopy (AFM), we describe a unique mechanism through which NRP-2 expressed on cancer cells interacts with α5 integrin on endothelial cells to mediate vascular adhesion and extravasation. Taken together, our studies reveal a clinically significant role of NRP-2 in cancer cell extravasation and promotion of metastasis. *Cancer Res; 73(14); 4579–90. ©2013 AACR.*

## Introduction

Tumor metastasis is the primary cause of mortality in patients with cancer (1) and occurs when a very small population primary tumor cells intravasate the walls of blood and/or lymphatic vessels, enter the circulation, arrest within capillaries, extravasate from the bloodstream, and colonize a distant organ (2). To effectively prevent and treat cancer metastasis, a detailed understanding of the molecular mechanisms that regulate the capillary extravasation of tumors cells from the primary site and subsequent metastatic invasion of distant organs is necessary. While this particular focus of cancer metastasis remains understudied, recent evidence suggests that neuropilins (NRP) may be involved in extravasation and metastatic invasion.

NRPs constitute a family of type I transmembrane proteins, including neuropilin-1 (NRP-1) and neuropilin-2 (NRP-2). Initially, NRP-1 and NRP-2 were discovered as class 3 semaphorin and vascular endothelial growth factor receptors (3–12). While NRP-1 and NRP-2 share 45% protein sequence homology in their protein sequences, some of their functions differ. NRP-1 homozygous knockout mice die at E12.5 to E13.5 with severe neural and vascular disorders (13), whereas homozygous NRP-2 mutant mice are viable, only showing minor defects in the neural and circulatory system (14–16). Given the more dispensable role of NRP-2 in neural and vascular development compared with NRP-1, less is known about its biologic properties.

Recent evidence suggests that NRP-2 is expressed in tumor tissue and plays a role in tumor progression and metastasis (17–20). NRP-2 is highly expressed on the surface of cancer cells from pancreatic neuroendocrine tumors (21), pancreatic ductal adenocarcinomas (22), and colorectal carcinomas (17), and NRP-2 expression on tumor cells cosegregated with poor prognosis in cohorts of patients with osteosarcoma (23) and breast cancer (24). NRP-2 expression also correlates with lymph node metastasis in breast cancer (24) and papillary thyroid carcinoma (20). However, the molecular mechanisms through which NRP-2 promotes tumor metastasis remain unknown, although several studies have implicated NRP-2 in

**Authors' Affiliations:** [1]Department of Biochemistry and Molecular Biology, College of Medicine, Mayo Clinic, Rochester, Minnesota; [2]Bioengineering Program & Department of Mechanical Engineering and Mechanics, Lehigh University, Bethlehem, Pennsylvania; [3]The Kinghorn Cancer Centre, Cancer Research Division, Garvan Institute of Medical Research; [4]Department of Surgery, Bankstown Hospital, Sydney; [5]South Western Sydney Clinical School, Faculty of Medicine, University of New South Wales, Liverpool, New South Wales; and [6]Queensland Centre for Medical Genomics, Institute for Molecular Bioscience, The University of Queensland, St. Lucia, Queensland, Australia

**Note:** Supplementary data for this article are available at Cancer Research Online (http://cancerres.aacrjournals.org/).

L.H. Hoeppner, S. Bach, and G. E contributed equally to this work.

**Corresponding Author:** Debabrata Mukhopadhyay, Department of Biochemistry and Molecular Biology, College of Medicine, Mayo Clinic, Guggenheim 13-21C, 200 First Street S.W., Rochester, MN 55905. Phone: 507-538-3581; Fax: 507-293-1058; E-mail: mukhopadhyay.debabrata@mayo.edu

**doi:** 10.1158/0008-5472.CAN-13-0529

Published OnlineFirst May 20, 2013; DOI: 10.1158/0008-5472.CAN-13-0529



the regulation of CXCR4 (24) and survival signaling (17, 22, 25). Therapeutically targeting NRP-2 expressed on tumor lymphatic endothelial cells through blocking antibody has shown some advantages, including inhibition of tumor lymphangiogenesis, thereby restricting tumor lymphogenous metastasis (18).

Here, we report that NRP-2 promotes cancer metastasis using renal cell carcinoma (RCC) and pancreatic cancer models. NRP-2 expressed on tumor cells functions as an adhesion molecule through a transinteraction with α5 integrin on the surface of endothelial cells. This interaction represents a potential mechanism through which NRP-2 promotes cancer metastasis.

## Materials and Methods

### Cell culture

Human RCC cell lines 786-O, A-498, 769-P, Caki-1, and Caki-2 were purchased from American Type Culture Collection (ATCC) and maintained according to their instructions. Normal kidney epithelial cell lines renal proximal tubular epithelial (RPTE), and HK-2 (ATCC) were maintained in keratinocyte serum-free medium (K-SFM) plus 0.05 mg/mL bovine pituitary extract (BPE) and 5 ng/mL human recombinant epidermal growth factor (EGF). Human umbilical vein endothelial cells (HUVEC; Lonza) were cultured in endothelial basal medium (EBM) supplemented with the EGM-MV Bullet Kit [5% fetal bovine serum (FBS), 12 μg/mL bovine brain extract, 1 μg/mL hydrocortisone, and 1 μg/mL GA-1000]. HUVEC of passage 3 to 5 were used throughout all experiments. Plates for HUVECs culture were always coated by bovine collagen type I (BD Biosciences). Pancreatic cancer cell line ASPC-1 (ATCC) was maintained in RPMI-1640 plus 10% FBS. All cell lines were certified by indicated cell bank and periodically authenticated by morphologic inspection.

As we found that NRP-2 is a trypsin-sensitive membrane protein, in all of the experiments we used 5 mmol/L EDTA/PBS to detach the cells from the culture plate.

### Antibodies

Western blot antibodies for NRP-2 (sc-5542), α2 integrin, α3 integrin, α5 integrin, α6 integrin, αV integrin, AKT, phosphor-AKT, phosphor-p38, phosphor-Erk1/2, p38, p53, and β-Actin were from Santa Cruz Biotechnology. Goat anti-GFP antibody was from Abcam. Mouse anti-HA antibody was from Sigma. Goat anti-NRP-2 antibody (AF-2215) for immunohistochemistry and blocking was from R&D Systems, Inc. α5 integrin antibody [Clone: 5H10-27(MFR5)] was purchased from Biolegend for blocking. For immunohistochemistry staining, anti-vWF antibody was from Millipore and anti-LYVE was from Angiobio. HRP-conjugated secondary antibodies were purchased from Santa Cruz Biotechnology.

### siRNA and shRNA

Human NRP-2 siRNA and control siRNA were purchased from Qiagen. siRNA transfection was carried out by Hiperfect from Qiagen; Lentiviral shRNA plasmids targeting human NRP-2 shRNAs and control plasmid were purchased from Open-Biosystems Inc. Lentivirus was prepared by transfecting the shRNA plasmid together with Gagpal and Vsvg plasmid into 293T cells. After 2 days of lentivirus infection, cells were selected by 2 μg/mL puromycin and stable selected cells were used in the following experiments.

The targeting sequences of human NRP-2 siRNA and shRNA are CAC AAA GAT TTA AAC AAG AAA and CCG TTT CCA GAT GAC AGG AAT T, respectively.

### Preparation of whole-cell extracts

Cells were washed twice with cold phosphate-buffered saline (PBS), lysed with ice-cold RIPA lysis buffer [50 mmol/L Tris (pH 7.5), 1% NP-40, 150 mmol/L NaCl, 0.5% sodium deoxycholate, 0.1% sodium dodecyl sulfate (SDS)] with 1% proteinase inhibitor cocktails (PIC; Sigma-Aldrich), and 1% Halt phosphatase inhibitor cocktail (Pierce), incubated on ice for 30 minutes, and centrifuged at 14,000 rpm at 4°C for 10 minutes. Supernatant was collected, and protein concentration was measured by Bradford method (Bio-Rad Protein Assay).

### Western blot

Proteins were denatured by adding 6× Laemmli SDS sample buffer and were heated for 4 minutes. Equal amounts of total protein per lane were subjected to SDS gel electrophoresis followed by wet transfer of the protein to polyvinylidene fluoride (PVDF) membrane. The membrane was blocked by incubation in TBS-T buffer (50 mmol/L tris-HCl, pH 7.4, 150 mmol/L NaCl, and 0.05% Tween 20) containing 5% nonfat milk or BSA. The primary antibody was diluted in TBS-T containing 5% nonfat milk or BSA overnight at 4°C, and horseradish peroxidase (HRP)-conjugated secondary antibody (Santa Cruz Biotechnology) was diluted in TBS-T and incubated for 1 hour at room temperature. Immunodetection was conducted with the SuperSignal West Pico Substrate (Thermo Scientific).

### Cell migration and invasion assay

Transwell chambers with a diameter of 6.5 mm and a pore size of 8 μm (Corning Costar Corporation) were used in the migration and invasion assay. For the migration assay, cells were detached from the plate by 5 mmol/L EDTA to avoid cleavage of any membrane proteins by trypsinization. The cells were resuspended in SFM and adjusted into $2 \times 10^5$ cells/mL. Cell suspension of 200 μL was added to the top chamber and serum containing medium of 600 μL was added to the bottom chamber of the transwells. The cells were then incubated for 2 hours at 37°C in a $CO_2$ incubator. Cells that remained in the top chamber were removed by gently scraping with a cotton swab. Cells that had invaded through the filter were fixed in 100% methanol and then stained with 0.2% crystal violet dissolved in 2% ethanol. Cells migrated through the membrane were counted by using bright-field optics with a Nikon Diaphot microscope equipped with a 16-square reticule (1 $mm^2$). Four separate fields were counted for each filter. The average of the 3 separate experiments has been documented.

The invasion assay was conducted similarly to the migration assay except that transwell chambers were precoated with 4 mg/mL Matrigel (BD Biosciences), and the incubation time was 6 hours.

Published OnlineFirst May 20, 2013; DOI: 10.1158/0008-5472.CAN-13-0529



### Cell proliferation assay

Cells ($1 \times 10^4$) were seeded into 24-well plates, subjected to the siRNA treatment, and cultured for 2 days in the complete medium. 1 μCi [$^3$H]-thymidine was added to each well and, 4 hours later, cells were washed with cold PBS, fixed with 100% cold methanol, and collected for the measurement of trichloroacetic acid-precipitable radioactivity.

### Cell adhesion assay

HUVECs were cultured in 6-well plate till confluency. In general $1 \times 10^5$ 786-O cells were resuspended into SFM and added onto HUVECs for 30 minutes at 37°C. Plates were washed by PBS gently to remove unadhered cells. Cells adhered on the HUVECs were counted under a ×4 microscope and 5 fields were taken for each well. In some cases, HUVECs or 786-O cells were preincubated with blocking antibodies (5 μg/mL) as indicated at 4°C for 30 minutes, and then cell adhesion assay was conducted.

### Zebrafish cancer cell extravasation model

Cancer cells were trypsinized, counted, and labeled with Cell Tracker Orange CMTMR (Invitrogen) according to the manufacturer's instructions. Cells were resuspended in PBS containing DNase I and heparin, and 50 to 200 cells were microinjected into the pericardium of anesthetized 3 dpf Tg(Fli-GFP) zebrafish. The zebrafish were put in 37°C embryo water for 24 hours following injection and then imaged on a ZEISS LSM 780 confocal microscope using standard FITC and dsRed filter sets.

### Plasmids

The following plasmids were used in this experiment: luciferase/EGFP in pSIN lentiviral vector; wild-type NRP-2 in pMMP retroviral vector; c-terminal HA-tagged NRP-2 in pMMP retroviral vector; c-terminal EGFP-tagged α5 integrin in pEGFP-N3 vector.

### Construction of the NRP-2 expression vector

NRP-2 cDNA in pcDNA3.1 plasmid was obtained from Dr. Shay Soker. The NRP-2 gene was subcloned into the pMMP retroviral vector by AgeI and BlpI. Virus preparation and cell infection were carried out as previously described (26).

### *In vivo* tumor model

***RCC subcutaneous model.*** Female 6-week-old nude mice were obtained from NIH. To establish tumor growth in mice, $2 \times 10^6$ cells, resuspended in 100 μL of PBS, were injected into the right flank of the mice subcutaneously. Tumors were measured every 2 weeks. Primary tumor volumes were calculated with the formula $V = 1/2a \times b^2$, where $a$ is the longest tumor axis, and $b$ is the shortest tumor axis.

Before the primary tumor reached a certain size (10% of the body weight), the mice were anaesthetized and the primary tumors were surgically removed. The mice were housed for another 4 to 6 months and were subjected to luciferase imaging.

Metastasis was monitored by the bioluminescence IVIS Imaging System 200 (Xenogen Corp.). Before imaging, animals were anesthetized with an intraperitoneal injection of ketamine/xylazine and injected intraperitonealy with 100 μL 40 mg/mL D-luciferin potassium salt in PBS. After 10 minutes of incubation with luciferin, digital image was acquired.

***Pancreatic cancer orthotopic model.*** Male 8-week-old SCID mice were obtained from NIH. Mice were anesthetized and $2 \times 10^6$ control shRNA or NRP-2 shRNA ASPC-1 cells, resuspended in 100 μL of PBS, were injected into the pancreas of the mice. After 15 days, mice were sacrificed and primary tumors were weighted and liver metastasis was imaged by IVIS Imaging System 200 by detecting the GFP signal.

The mice were housed in the institutional animal facilities. All animal work was conducted under protocols approved by the Mayo Clinic Institutional Animal Care and Use Committee.

### Immunohistochemistry staining

Tumors were removed and fixed in neutral buffered 10% formalin at room temperature for 24 hours before embedding in paraffin and sectioning. Sections were deparaffinized and then subjected to vWF and LYVE immunochemistry staining. Stable diaminobenzidine was used as a chromogen substrate, and the sections were counterstained with a hematoxylin solution.

Patient RCC tissue microarrays (TMA) were brought from BioMax, Inc. NRP-2 staining was conducted by using goat anti-NRP-2 antibody and anti-goat immunostaining kit from R&D systems.

### Expression array and survival analysis

The gene expression data is from The International Cancer Genome Consortium (ICGC) pancreatic cancer project that is stored at Gene Expression Omnibus (GEO) with accession number GSE36924. It includes gene expression data from 90 primary tumor samples, 88 of which contain patient outcome, and was used in the survival analysis according to previously described methods (27). To confirm the microarray probe quality, we: aligned the probe sequences to the genome using UCSC BLAT (28); and also used an Illumina reannotation pipeline (29). Both methods confirmed that the probes for NRP1 and NRP2 perfectly and uniquely matched the 3′ end of the intended gene, though both genes have a number of splice isoforms.

### 786-O cell–HUVEC adhesion measured by Atomic Force Microscopy

Atomic Force Microscopy (AFM) is a technique to measure the mechanical contact force between cells. We used AFM to measure the interaction between cancer cells and endothelial cells mediated by NRP-2. As illustrated in Fig. 6A, AFM measurement of the interaction between an individual 786-O cell and a HUVEC involves a series of 4 steps. The cantilever with an attached 786-O cell is first lowered onto a HUVEC. Following a 1-second contact at a compression force of 500 pN, the cantilever is subsequently retracted, pulling the 786-O–HUVEC pair apart until complete separation of the 2 cells is achieved. During this process, the AFM continuously monitors the force of the cantilever to report on the interaction between the 786-O cell and the HUVEC. A typical AFM retraction trace is presented in Fig. 6B. Upon retraction of the cantilever, molecular

Published OnlineFirst May 20, 2013; DOI: 10.1158/0008-5472.CAN-13-0529



linkages established between the cells pulled the cantilever downward. The cell detachment process typically involved a series of rupture events, as indicated by arrows (Fig. 6B), and may correspond to the detachment of one or more adhesive ligand–receptor bonds. We measured the "detachment work," which is derived from integrating the adhesive force over the distance traveled by the cantilever up to the point of the last bond rupture (shaded area in Fig. 6B; refs. 30–32). As previously described (32–34), HUVECs were plated on standard 35-mm tissue culture dishes, whereas a single 786-O cell was coupled to the end of the AFM cantilever (MLCT, Bruker Nano) (Fig. 6A). Cantilevers were individually calibrated using the equipartition theorem (35) and had spring constants ranging from 0.015 to 0.025 N/m. The AFM force measurements were carried out by a custom-built AFM with individual 786-O cells attached to the tip of an AFM cantilever via a Concanavalin A (Con A)–mediated linkage (33, 34). Measurements of 786-O–endothelial cell interactions were conducted at 25°C in EBM. At the onset of the measurements, the 786-O cells coupled to the AFM cantilever were positioned directly above the either center of an isolated HUVEC, or a HUVEC–HUVEC cell junction in a Petri dish seeded with HUVECs to approximately 50% confluency.

### Statistical analysis

Statistical analysis was conducted by *t* test or ANOVA, with *P* less than 0.05 considered statistically significant. The data were presented as means ± SD or SEM as indicated in the results.

## Results

### NRP-2 depletion does not affect primary tumor growth but decreases metastasis in a RCC xenograft tumor model

We previously showed NRP-1 controls tumorigenesis in RCC (36). Here, NRP-2 protein expression was examined in RCC cell lines. Similar to the NRP-1 expression profile, NRP-2 is expressed at greater levels in aggressive RCC cell lines (786-O, A-498, and Caki-1) compared with less aggressive RCC and normal kidney epithelial cell lines (769-P, Caki-2, HK-2, and RPTE cell; Fig. 1A).

To explore the role of NRP-2 in the tumorigenic ability of cancer cells, we used an *in vivo* xenograft tumor model by

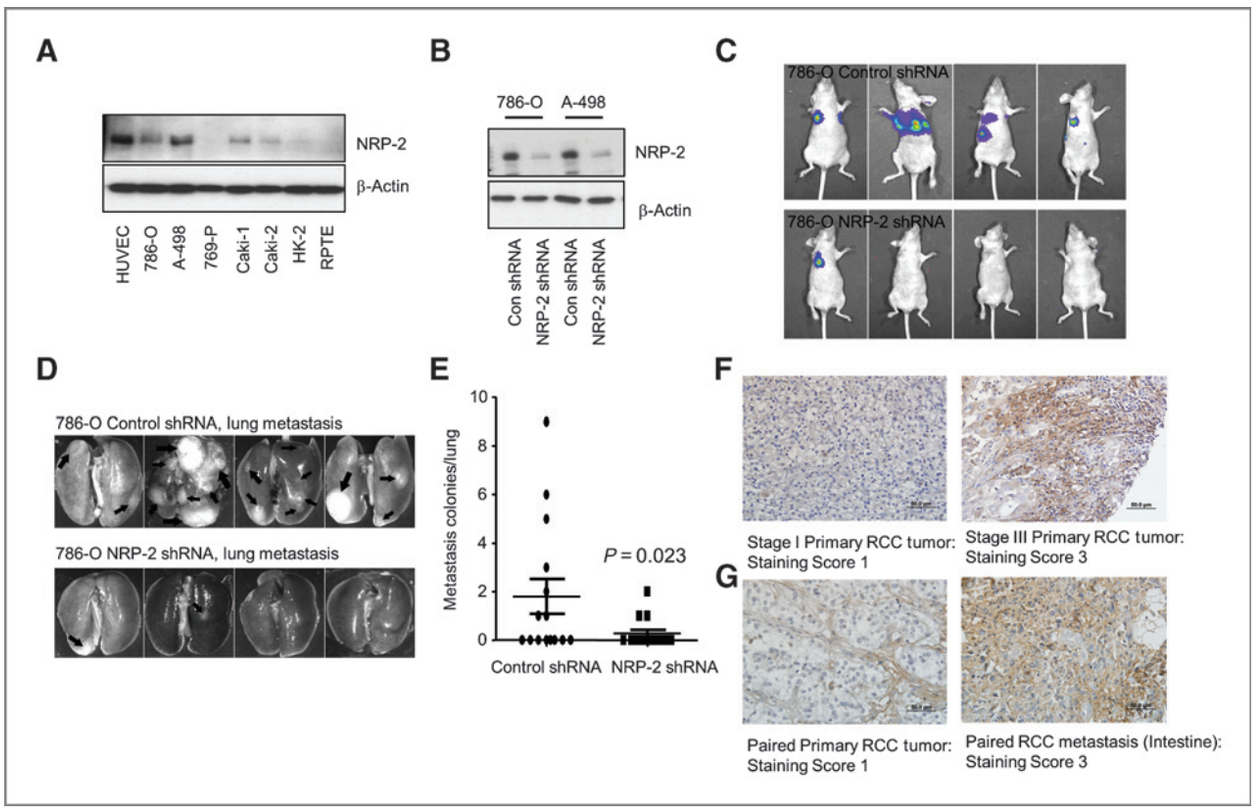


Figure 1. The impact of NRP-2 on RCC tumorigenesis and lung metastasis. A, NRP-2 expression levels were compared by Western blotting among RCC and normal renal epithelial cell lines, including 786-O, A-498, 769-P, Caki-1, Caki-2, HK-2, and RPTE. HUVECs cell lysate was used as a positive control. B, NRP-2 expression was knocked down by NRP-2 shRNA in 786-O and A-498 cells. Knockdown efficiency was determined by Western blotting. C and D, lung metastasis was significantly reduced in 786-O NRP-2 knockdown group compared with control group. C, representative luciferase images of metastasis from control (top) and NRP-2 knockdown (bottom) animals. D, representative images of lungs from control (top) and NRP-2 knockdown (bottom) animals. E, quantification of the number of metastatic nodules per lung ($P = 0.023$). F, immunohistochemistry for NRP-2 on TMA containing 85 stage I, 57 stage II, 29 stage III, and 7 stage IV tumor tissue samples from patients with ccRCC. Left, stage I primary RCC tumor sample (staining score 1); right, stage III primary RCC tumor sample (staining score 3). G, immunohistochemistry for NRP-2 on metastatic and their counterpart primary tumor TMA of patients with RCC ($n = 8$). Left, primary RCC tumor sample (staining score 1). Right, metastatic RCC sample matching for the left (staining score 3).

Published OnlineFirst May 20, 2013; DOI: 10.1158/0008-5472.CAN-13-0529



injecting tumor cells subcutaneously into nude mice. First, we knocked down NRP-2 expression in 786-O and A-498 cells using lentivirus-mediated shRNA and assessed knockdown efficiency by Western blotting (Fig. 1B, Supplementary Fig. S1A). Next, $2 \times 10^6$ control or NRP-2 knockdown cells were injected subcutaneously into female nude mice. Unexpectedly, we did not observe significant differences in the primary tumor growth rate between control and NRP-2 knockdown in either 786-O or A-498 cells ($n = 15$ and 5, respectively; Supplementary Fig. S1B and S1C). We continued to monitor the 786-O tumor burden mice for 4 months following the required removal of primary tumors that had surpassed the maximum allowable size. Interestingly, we found that in the 786-O NRP-2 shRNA group, the mice showed much less lung metastasis (3 in 15) than those in the control shRNA group (7 in 15; Fig. 1C). Furthermore, the metastasis nodules on the lung were significantly less in NRP-2 knockdown group ($1.80 \pm 0.72$ vs. $0.27 \pm 0.15$ for 786-O Control shRNA versus 786-O NRP-2 shRNA; $P = 0.023$. Mean $\pm$ SEM; $n = 15$; Fig. 1D and E). Taken together, these findings suggest that NRP-2 promotes RCC lung metastases.

Lung is a common site of RCC metastasis, occurring in 50 to 60% of patients with RCC with metastases (37). RCC metastasis usually occurs through hematogenous spread to the lung parenchyma and less frequently involves the lymphogenous route (38). Therefore, we sought to determine whether the decreased metastasis we observed upon NRP-2 knockdown was the result of reduced blood or lymphatic vessels in the primary tumor. Thus, we conducted pathologic examination of blood and lymphatic vessel density in the primary tumor using vWF and LYVE staining and found no significant difference in tumors derived from 786-O control shRNA cells compared with tumors formed from 786-O NRP-2 shRNA cells (Supplementary Fig. S2A–D).

### High NRP-2 expression in patients with RCC is associated with advanced tumor stage

To access the relativity between NRP-2 expression and tumor progression in patients with RCC, we explored the NRP-2 expression pattern in clear cell RCC (ccRCC) patient samples using paraffin-embedded TMA. This TMA contained 85 stage I, 57 stage II, 29 stage III, and 7 stage IV ccRCC tumor tissue samples. NRP-2 staining intensities of the tumor tissue were scored as 0 (no staining), 1 (weak staining), 2 (moderate staining), and 3 (strong staining). The NRP-2 levels were significantly higher in the stage III and IV ($n = 36$) ccRCC samples than in stage I and II tissue ($n = 142$; $P = 0.002$; Fig. 1F), suggesting that NRP-2 expression correlates with advanced tumor stage.

### NRP-2 expression in metastasis is higher than in primary RCC tumors

Next, we used another RCC TMA, which contained 8 primary RCC tumor samples as well as matched tumor samples from metastatic sites, including lung, intestine, lymph node, spleen, bone, adrenal gland, and thyroid. NRP-2 staining intensities were scored as described above. NRP-2 expression was found to be significantly higher in the matched metastatic carcinoma than the primary tumors ($P = 0.0062$, $n = 8$; Fig. 1G), which supports our finding that NRP-2 promotes cancer metastasis.

### NRP-2 knockdown does not affect cancer cell migration and invasion *in vitro*

NRP-2 has been shown to regulate cellular proliferation, migration, and invasion by other groups using a variety of cell lines. Therefore, we assessed these cellular processes in NRP-2 knockdown 786-O and A498 cells to better understand the mechanism through which NRP-2 mediates tumor metastasis. None of these cellular behaviors were significantly changed after NRP-2 depletion (Supplementary Fig. S3A). We further examined classical cell survival and proliferation signaling pathways such as phospho-Akt, phospho-MAPK, phospho-p38, and p53 levels. Again, no significant changes were observed following NRP-2 knockdown in 786-O and A-498 cells (Supplementary Fig. S3B).

### NRP-2 promotes extravasation of 786-O cells in zebrafish

In general terms, the tumor metastasis process consists of the following steps: (i) the intravasation of tumor cells from the primary site; (ii) the migration of tumor cells through the bloodstream, (iii) vascular adhesion of tumor cells within distant capillaries, and (iv) the extravasation of tumor cells from the bloodstream to invade and colonize a distant metastatic site. To evaluate whether NRP-2 promotes extravasation of tumor cells, we used an *in vivo* cancer metastasis extravasation model (39). Control and NRP-2 overexpressing 786-O cells (Fig. 1B) were labeled with a red tracker dye and microinjected into the pericardium of 3 days postfertilization (dpf) Tg(fli-GFP) zebrafish embryos. After 24 hours, we observed NRP-2 overexpressing 786-O cells in the extravascular space, whereas control 786-O cells remained in the intersegmental vessels (ISV; Fig. 2A and B, E and F). Furthermore, we captured NRP-2 overexpressing 786-O cells actively extravasating from the ISV, but no similar extravasation events were seen in zebrafish injected with control 786-O cells (Fig. 2C and D, G and H). Together, these findings indicate that NRP-2 promotes extravasation of tumor cells.

### Surface expression of NRP-2 on cancer cells mediates their adhesion to endothelial cells

Cell–cell interactions of cancer cells with the endothelium mediate the metastatic spread. Given that NRP-1 was first discovered as an adhesion molecule, we sought to determine whether NRP-2 expressed on the surface of cancer cells could mediate an interaction between cancer cells and endothelial cells. We hypothesized that this transinteraction may promote the homing of cancer cells to the endothelium of a target organ, thus promoting extravasation of tumor cells and facilitating tumor metastasis. Through use of *in vitro* cell adhesion assay, indeed, we observed that overexpression of NRP-2 in 786-O cells enhanced their adhesion to an endothelial monolayer, whereas knockdown of NRP-2 impaired the ability of 786-O cells to adhere to endothelial cells (Fig. 2I). Adhesion of 786-O cells to an uncoated or collagen I-coated plate was unaffected by NRP-2 overexpression or depletion (Supplementary Fig. S4A and S4B). Furthermore, the NRP-2 blocking antibody modestly

Published OnlineFirst May 20, 2013; DOI: 10.1158/0008-5472.CAN-13-0529



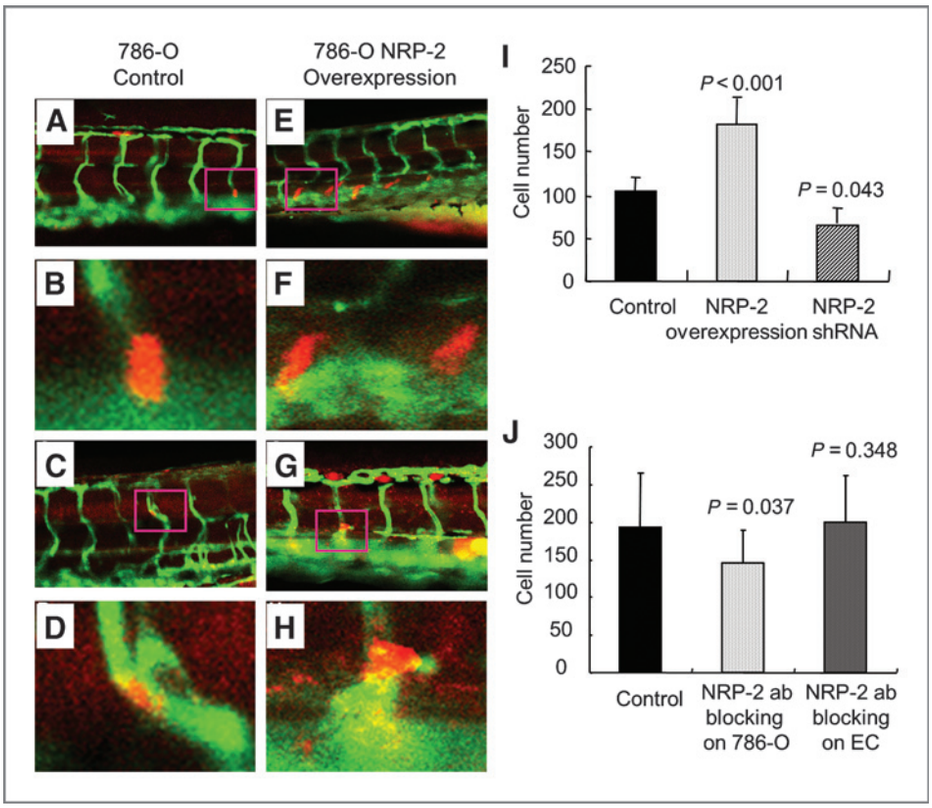


Figure 2. NRP-2 promotes extravasation of 786-O cells in a zebrafish model and endothelial adhesion *in vitro*. Control (A–D) and NRP-2–overexpressing (E–H) 786-O cells were microinjected into the pericardium of 3 dpf Tg(Fli-GFP) zebrafish and imaged 24 hours later. A–D, control 786-O cells remain in circulation within the ISVs. E and F, NRP-2–overexpressing 786-O cells that have extravasated from the ISV. G and H, NRP-2–overexpressing 786-O cells actively extravasating from the ISV. I, overexpression or knockdown of NRP-2 in 786-O cells, respectively, enhanced or impaired its adhesion ability to the endothelial monolayer. J, preblocking NRP-2 on 786-O cells significantly impaired 786-O adherence to HUVEC monolayer. Preblocking NRP-2 on HUVEC did not significantly affect 786-O adherence to the HUVEC monolayer.

impaired the cancer cell-endothelial cell interaction; whereas pretreating endothelial cells with anti-NRP-2 antibody did not inhibit their adhesion to cancer cells, despite relatively equal levels of NRP-2 expression in HUVEC cells and 786-O cells (Figs. 2J and 5B). The NPR-2 blocking antibody only exhibits partial blocking at the concentration we used (5 μg/mL), which may explain the moderate effect. These results suggest that NRP-2 mediates adhesion through an NRP-2 transinteracting partner that is highly expressed on endothelial cells but has little to no expression on 786-O cells.

### NRP-2 also promotes cell–cell adhesion, extravasation, and cancer metastasis *in vivo* in a pancreatic cancer model

To extend our findings to other types of cancer cells, we used ASPC-1, a highly metastatic pancreatic cancer cell line, to test our hypothesis that NRP-2 promotes cancer metastasis by mediating cancer cell-endothelial cell adhesion. ASPC-1 express high levels of NRP-2, which was knocked down by shRNA (Fig. 3A). NRP-2 knockdown reduced ASPC-1 adhesion ability to an endothelial monolayer *in vitro* (Fig. 3B). Using the zebrafish extravasation model as described previously, NRP-2 knockdown ASPC-1 cells (Fig. 3G–J) also showed less extravasation ability compared with control cells (Fig. 3C–F). Similar to the RCC xenograft results, NRP-2 knockdown in ASCP-1 cells did not significantly reduce the primary tumor growth (441.4 ± 135.3 mg vs. 340.1 ± 121.1 mg; $P = 0.095$ for ASPC-1 Consh vs. ASPC-1 NRP-2sh, respectively; mean ± SD, $n = 10$; Supplementary Fig. S5A), but significantly reduced cancer cell liver metastasis in a SCID mouse xenograft model (Fig. 3K and L; Supplementary Fig. S5B).

### High NRP-2 expression is cosegregated with poor patient survival in pancreatic cancer

To gain insight into the clinicopathologic significance of these findings, we first characterized the expression profile of NRP-1 and NRP-2 mRNA transcripts in a prospectively acquired cohort of patients with pancreatic cancer (27). NRP-1 was detected in all samples and expression varied over the cohort in a continuous fashion, whereas NRP-2 expression was only detected in 20% of tumors when compared with background. Next, the cohort was dichotomized into low- and high-expression groups and a log-rank test was conducted to compare survival. NRP-1 expression did not correlate with patient prognosis (Fig 4A). However, use of a 20:80% (high:low) cut-off revealed high expression of NRP-2 cosegregated with poor patient survival ($P = 0.0001618$; HR 4.315; 95% CI: 1.894–9.833; Fig 4B).

Overall, our data from preclinical models of RCC and pancreatic cancer, and corresponding patient cohorts, support a prominent role for NRP-2 in metastasis of different cancer types.

### Transinteraction between NRP-2 and α5 integrin

Given the key role integrins play in mediating tumor metastasis (40), we hypothesized that an integrin expressed on the surface of endothelial cells may interact with NRP-2 on cancer cells to promote metastasis. To address this hypothesis, we

Published OnlineFirst May 20, 2013; DOI: 10.1158/0008-5472.CAN-13-0529



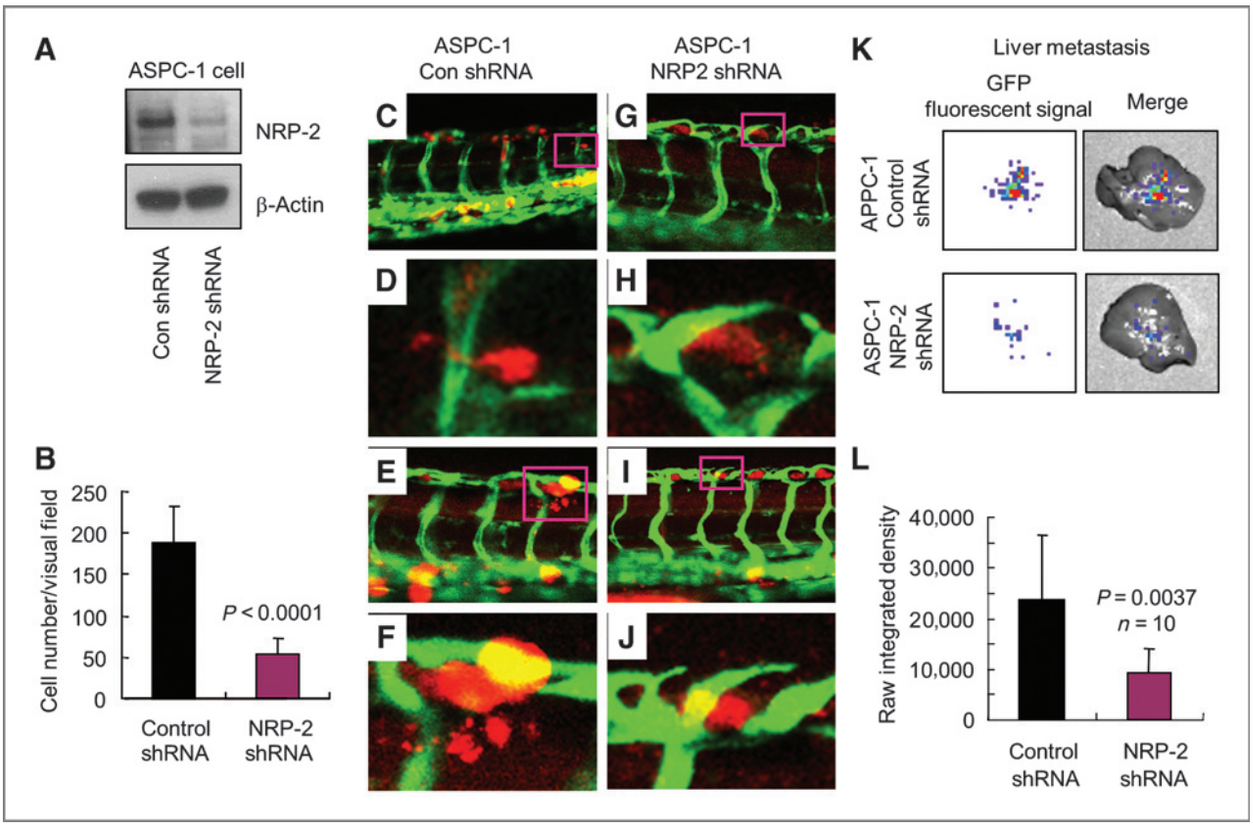


Figure 3. NRP-2 promotes cell–cell adhesion, extravasation, and cancer metastasis *in vivo* in a pancreatic cancer model. A, NRP-2 was knocked down in ASPC-1 cell by shRNA. B, NRP-2 knockdown significantly reduced ASPC-1 cell adhere to the endothelial monolayer. C–H, NRP-2 knockdown reduced extravasation of ASPC-1 cells in a zebrafish model. Control (C–F) and NRP-2 knockdown (G–J) ASPC-1 cells were microinjected into the pericardium of 3 dpf Tg(Fli-GFP) zebrafish and imaged 24 hours later. C and D, control ASPC-1 cells that have extravasated from the ISVs. E and F, control ASPC-1 cell actively extravasating from the ISV. G–J, NRP-2 knockdown ASPC-1 remain in circulation within the ISV. K, representative images of livers from control and NRP-2 knockdown ASPC-1 tumor burden mice. The cells were transfected with GFP and the GFP fluorescent signal was examined by IVIS Imaging System 200. L, quantification of liver metastasis by quantification of the GFP signal intensity. NRP-2 knockdown reduced ASPC-1 cell metastasis to the liver.

immunoprecipitated NRP-2 from confluent 786-O and HUVEC coculture cell lysate and found NRP-2 and α5 integrin immunoprecipitate together in a complex (Fig. 5A and B), whereas NRP-2 did not immunoprecipitate with α2, α3, α6, or αV integrins (Supplementary Fig. S6). To determine whether the interaction between NRP-2 and α5 integrin is a *cis* or *trans*-binding, we transfected 293T cells with C-terminal HA-tagged NRP-2 and C-terminal GFP-tagged α5 integrin separately, cocultured them, and conducted immunoprecipitation with the resulting lysate. Through immunoprecipitation with an anti-HA antibody followed by Western blotting for GFP and integrin α5, we detected an interaction between NRP-2 and α5 integrin (Fig. 5C and D). We also *in situ* crosslinked the protein using DSP crosslinker and conducted immunoprecipitation with anti-HA antibody and blotted with GFP and α5 integrin. This time, NRP-2 and α5 integrin we detected a complex at a molecular weight slightly higher than 250 kDa, which is indicative of NRP-2 (120 kDa) and α5 integrin (150 kDa) coimmunoprecipitating (Fig. 5E). We found that pretreatment of endothelial cells with anti-α5 integrin blocking antibody modestly decreased 786-O and HUVEC adhesion, whereas pretreating 786-O cells with anti-α5 integrin antibody did not have a significant effect on adhesion (Fig. 5F). These results coincide with our findings that HUVEC cells have much higher α5 integrin expression than 786-O cells (Fig. 5B). Furthermore, pretreating endothelial cells with anti-α5 integrin blocking antibody eliminated their enhanced adhesion to NRP-2 overexpressing 786-O cells (Fig. 5G). Together, these results suggest that α5 integrin is a *trans*-binding partner for NRP-2.

### Quantification of cancer–endothelial cell interaction mediated by NRP-2

To quantify the adhesion between 786-O and HUVEC, we measured the detachment work of HUVEC bound to 786-O control, NRP-2 knockdown or overexpressing 786-O cells (Fig. 6C). In general, HUVEC cell–cell junctions are about 40% to 60% more adhesive to the 786-O. Compared with NRP-2 knockdown cells, an approximately 200% increase ($P < 0.05$) of detachment work was detected on NRP-2 overexpressed cells. Anti-α5 integrin antibody has a profound impact on 786-O–HUVEC adhesion. In both HUVEC bodies and cell junctions,

Published OnlineFirst May 20, 2013; DOI: 10.1158/0008-5472.CAN-13-0529



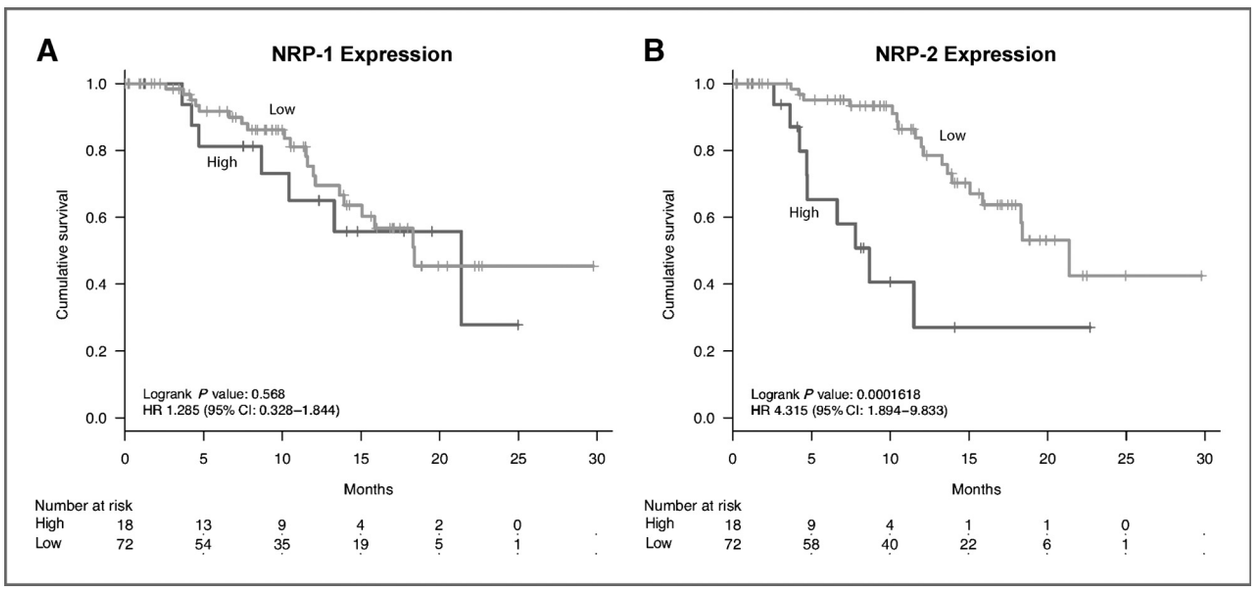


**Figure 4.** Prognostic significance of NRP-1 and NRP-2 expression in pancreatic cancer. A, Kaplan–Meier survival curves for patients stratified on the basis of NRP-1 mRNA expression in the prospectively accrued ICGC cohort ($n = 88$) using the 80% low: 20% high cutoff to match that used for NRP-2 (no correlations to patient survival were detected using a range of cut-offs). B, Kaplan–Meier survival curves for patients stratified on the basis of NRP-2 mRNA expression showing high NRP-2 expression cosegregated with poor patient survival.

incubation of the HUVEC cells with the antibody completely diminished the enhanced adhesion induced by NRP-2 overexpression. In addition, α5 integrin blockages also inhibited adhesion between 786-O control cells and HUVEC cell junctions (Fig. 6C, bottom). In ASPC-1 pancreatic cancer cells, NRP-2 knockdown significantly decreased detachment work of HUVEC junctions and anti-α5 integrin antibody abrogated ASPC-1–HUVEC adhesion in bodies and junctions (Fig. 6D). These findings suggest that NRP-2 is an adhesion molecule that could promote the adhesion between cancer cell and endothelial cell and α5 Integrin is a transbinding partner of NRP-2.

## Discussion

In this report, we show that NRP-2 promotes metastasis of RCC and pancreatic cancer in mouse and zebrafish models and describe a mechanism through which NRP-2 expressed on cancer cells interacts with α5 integrin on endothelial cells to mediate vascular adhesion and extravasation. Based on our work and other recent studies suggesting a link between NRP-2 expression levels and cancer metastasis (20, 24, 41), NRP-2 may represent a promising therapeutic target for preventing metastatic progression in patients with cancer. Caunt and colleagues have shown that a therapeutic NRP-2 blocking antibody reduces lymphatic vessels in tumor and resulted in a reduction in metastasis to the sentinel lymph node (18). They also observed decreased lung metastasis after NRP-2 antibody treatment, which was generally mediated through hematogenous spread and may not be explained by the reduction of lymphatic vessels. Therefore, blocking NRP-2 may represent a means to inhibiting the ability of cancer cells to adhere to the endothelium, thus preventing cancer colonization in the target organ. Our clinical results indicating that NRP-2 is upregulated in metastatic RCC tumors and correlates with a markedly worse prognosis in pancreatic cancer provide further evidence that NRP-2 represents a therapeutic target that warrants additional pursuit.

We previously reported that NRP-1 drives primary tumorigenesis in RCC (36). Here we show that, unlike NRP-1, NRP-2 does not promote primary tumor growth in RCC. Correspondingly, others have reported that NRP-2 drives aggressive prostate cancer (42) and, as discussed above, lymphatic metastases (18). Given that K-ras mutations usually do not occur in RCC, we confirmed that NRP-2 promotes metastasis in pancreatic cancer, which displays a high frequency of K-ras mutations. However, another study suggests that NRP-2 has a role in primary pancreatic tumor growth (22). One potential explanation for these disparate results could stem from differences in the human pancreatic cancer cell lines used for the mouse xenograft models. We used ASPC-1 cells, which possess a K-ras mutation, whereas the Dallas and colleagues report relied on wild-type K-ras BxPC3 cells.

To date, most studies of the adhesion properties of NRPs focused on NRP-1. NRP-1 was discovered initially as a cell to cell adhesion molecule (4), and b1b2 domain is responsible for this adhesion ability (43). The protein interacting in a transbinding manner with NRP-1 was reported to be a trypsin sensitive membrane protein, however, it has not been defined yet (43). NRP-1 also has been implicated in mediating cell to extracellular matrix adhesion (44). NRP-1 could form a complex with other membrane proteins such as α5 integrin (45), and β1 integrin (46) in a *cis*-binding fashion, and this could promote NRP-1–mediated cell–cell and cell–matrix adhesion. NRP-1 can also interact with L1CAM, a cell adhesion protein in both *cis* and *trans*-binding manner (47, 48). One observation that NRP-1 expressed on stromal cells supports hemotogenesis

Published OnlineFirst May 20, 2013; DOI: 10.1158/0008-5472.CAN-13-0529



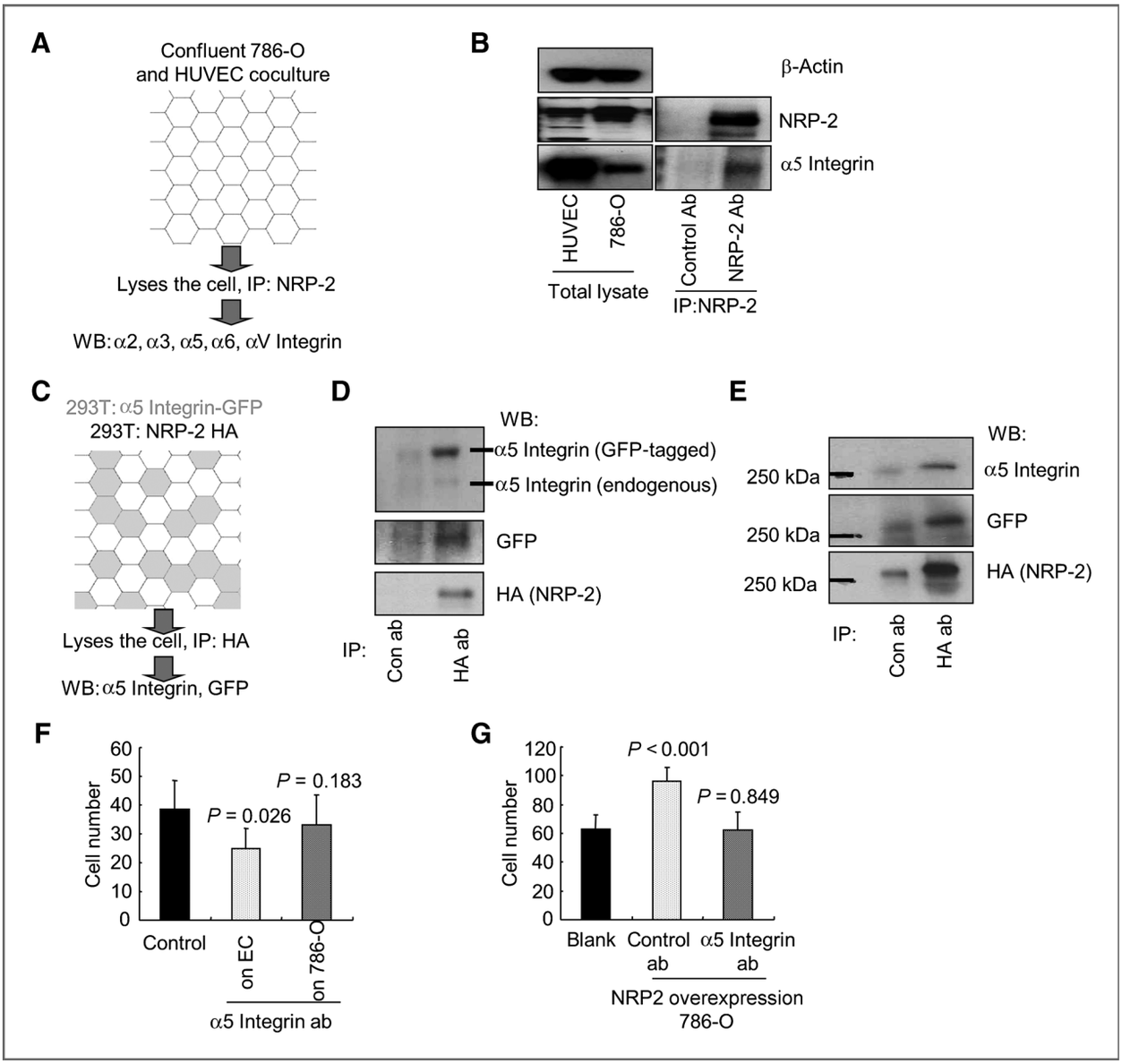


Figure 5. α5 integrin is a transbinding partner of NRP-2. A and B, α2, α3, α5, α6, and αV integrins were checked in the NRP-2 coimmunoprecipitation complex from confluent 786-O cell and HUVEC coculture. Only α5 integrin existed in the NRP-2 coimmunoprecipitation complex. C–E, α5 integrin–GFP protein was checked in the NRP-2 coimmunoprecipitation complex from confluent 293T cells transfected with GFP-tagged α5 integrin and 293T cells transfected with HA tagged with NRP-2. α5 integrin-GFP existed in the NRP-2-HA coimmunoprecipitation complex either noncrosslink (D) or crosslink (E). F, preblocking α5 integrin on HUVEC significantly impaired 786-O adherence to HUVEC monolayer. Preblocking α5 integrin on 786-O did not significantly affect 786-O adherence to HUVEC monolayer. G, preblocking α5 integrin on HUVEC reversed 786-O adherence to HUVEC monolayer enhanced by NRP-2 overexpression on 786-O cells.

also indicated that NRP-1 can function by *trans*-interaction with other cells (49).

NRP-2 has 45% similarity with NRP-1 and recently NRP-2 was shown to pair with α6β1-integrin in a *cis*-binding manner to mediate cell–matrix (laminin) adhesion (50). In this report, we discovered that NRP-2 on the cancer cells also possessed the cell–cell adhesion property and that the α5 integrin on the endothelial cells is the transbinding protein. We used AFM to precisely measure the attachment and detachment of cancer cells to endothelial cells via NRP-2 binding to α5 integrin and showed that addition of anti-α5 integrin antibody prevented interaction. We found that α5 integrin is not trypsin sensitive, but NRP-2 as well as NRP-1 is trypsin sensitive. It is possible that NRP-2 and NRP-1 have different or multiple *trans*-binding partner proteins. The beta-propeller domain of α integrin has similarity with sema domain of semaphorins and plexins (51, 52), which may provide the structural basis of *trans*-interaction between integrin and NRPs and warrants further investigation. Given that NRP-2 is also expressed on vein endothelial cells as well as lymphatic endothelial cells (16), it could be envisioned

Published OnlineFirst May 20, 2013; DOI: 10.1158/0008-5472.CAN-13-0529



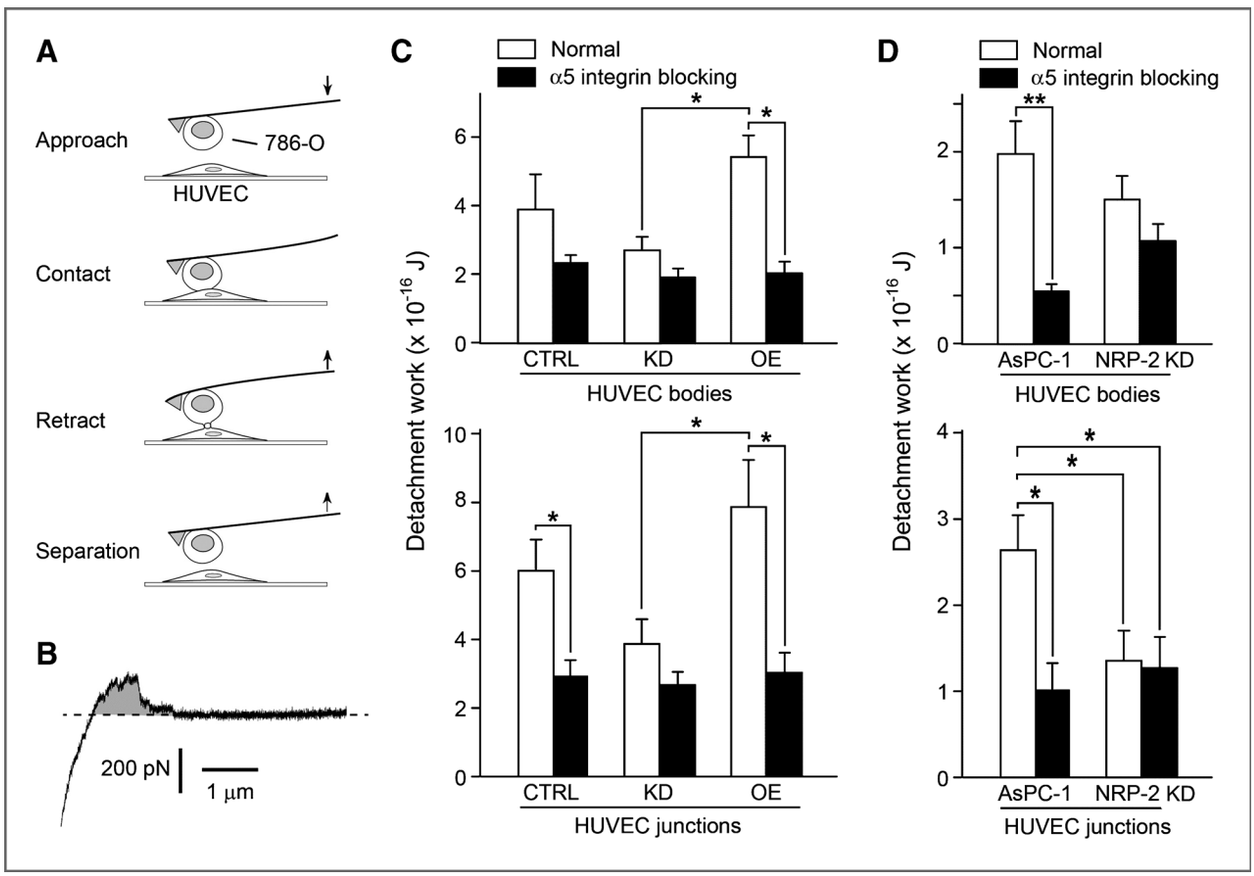


**Figure 6.** AFM measurements of 786-O/HUVEC interaction. A, schematic representation of a typical cycle of the AFM measurement: (i) approach of the 786-O cell to HUVEC, (ii) contact between 786-O and HUVEC, (iii) retraction of the 786-O, and (iv) separation of the 786-O from HUVEC. Arrows indicate the direction of cantilever movement. B, typical force spectrum retraction trace for a 786-O cell bound to HUVEC cell body. Measurements were acquired with a compression force of 500 pN, 1-second contact, and a cantilever retraction speed of 3.5 mm/s. Shaded area in the trace is the "detachment work." Arrows point to rupture events, i.e., breakage of adhesive bond(s). Dashed line indicates zero forces. C, adhesion strength between a single pair of a 786-O cell and HUVEC (top, HUVEC body; bottom, HUVEC cell junctions) measured by the detachment work. Experimental conditions were the same as in B. D, adhesion strength between a single pair of ASPC-1 cell and HUVEC (top, HUVEC body; bottom, HUVEC cell junctions) measured by the detachment work. The error bar is SE with $n > 5$ in each case. $^{*}$, $P < 0.05$ and $^{**}$, $P < 0.01$ between the indicated groups. CTRL, control 786-O; KD, NRP-2 knockdown; OE, NRP-2 overexpression.

that endothelial NRP-2 also interacts with cancer cell α5 integrin to promote cancer cell adhesion, though we report here that the RCC cell lines express much less α5 integrin than endothelial cells. In α5 integrin expressing MDA-MB-231 breast cancer cells, α5 integrin promoted lung metastasis in both a spontaneous and experimental lung metastasis model (53), and endothelial NRP-2 may contribute to these observed effects.

Through the use of several preclinical models, we show that NRP-2 contributes to cancer metastasis by mediating adhesion to endothelial cells through α5 integrin, and our data from clinical cohorts support a role for NRP-2 in metastatic progression. Adherence to endothelium enables tumor cells to subsequently extravasate from the bloodstream, and invade distant metastatic sites. Our finding is clinically significant because recent studies have shown the efficacy of NRP-2 blocking antibody as a potential therapy designed to block tumor metastasis (18). NRP-2 blocking antibody would prevent NRP-2 expressed by cancer cells from interacting with α5 integrin expressed on the surface of endothelial cells, thus inhibiting cancer cell adhesion to the endothelium, the initial event in tumor cell extravasation, a critical step in metastasis. Development of therapies to block NRP-2 represents a promising new direction to prevent cancer progression and metastasis and improve the clinical outcome of patients with cancer.

## Disclosure of Potential Conflicts of Interest

No potential conflicts of interest were disclosed by the authors.

## Authors' Contributions

**Conception and design:** Y. Cao, G. E, D.K. Chang, A.V. Biankin, D. Mukhopadhyay

**Development of methodology:** Y. Cao, L. Hoeppner, G. E, D.K. Chang, A.V. Biankin, X. Zheng

**Acquisition of data (provided animals, acquired and managed patients, provided facilities, etc.):** Y. Cao, L. Hoeppner, S. Bach, Y. Guo, D.K. Chang, S.M. Grimmond, A.V. Biankin

**Analysis and interpretation of data (e.g., statistical analysis, biostatistics, computational analysis):** Y. Cao, L. Hoeppner, S. Bach, Y. Guo, J. Wu, M.J.

Published OnlineFirst May 20, 2013; DOI: 10.1158/0008-5472.CAN-13-0529



Cowley, D.K. Chang, N. Waddell, S.M. Grimmond, A.V. Biankin, R.J. Daly, X. Zheng, D. Mukhopadhyay

**Writing, review, and/or revision of the manuscript:** Y. Cao, L. Hoeppner, S. Bach, Y. Guo, J. Wu, D.K. Chang, S.M. Grimmond, A.V. Biankin, R.J. Daly, X. Zheng, D. Mukhopadhyay

**Administrative, technical, or material support (i.e., reporting or organizing data, constructing databases):** E. Wang, D.K. Chang, D. Mukhopadhyay

**Study supervision:** A.V. Biankin, D. Mukhopadhyay

## Acknowledgments

The authors thank the Mayo Clinic Zebrafish Core Facility and Optical Morphology Facility for their assistance with this work. They also thank C. Axford, D. Gwynne, M.-A. Brancato, S. Rowe, M. Thomas, S. Simpson, and G. Hammond for central coordination of the Australian Pancreatic Cancer Genome Initiative, data management and quality control; M. Martyn-Smith, L. Braatvedt, H. Tang, V. Papangelis, and M. Beilin for biospecimen acquisition; and W. Waterson, J. Shepperd, E. Campbell, and E. Glasov for their efforts at the Queensland Centre for Medical Genomics.

## Grant Support

This work was partly supported by CA78383 and CA150190, and the Bruce and Martha Atwater Foundation (D. Mukhopadhyay) and grant No. 31101016 (Y. Cao) from the National Natural Science Foundation of China. D. Mukhopadhyay is a visiting professor at King Saud University (Riyadh, Saudi Arabia). L.H. Hoeppner is a fellow of NCI-T32 CA148073 and 13POST14510025 from the American Heart Association.

The costs of publication of this article were defrayed in part by the payment of page charges. This article must therefore be hereby marked *advertisement* in accordance with 18 U.S.C. Section 1734 solely to indicate this fact.

Received February 19, 2013; revised April 23, 2013; accepted May 3, 2013; published OnlineFirst May 20, 2013.

## References

1. Fidler IJ. The pathogenesis of cancer metastasis: the 'seed and soil' hypothesis revisited. Nat Rev Cancer 2003;3:453–8.
2. Gupta GP, Massague J. Cancer metastasis: building a framework. Cell 2006;127:679–95.
3. Takagi S, Hirata T, Agata K, Mochii M, Eguchi G, Fujisawa H. The A5 antigen, a candidate for the neuronal recognition molecule, has homologies to complement components and coagulation factors. Neuron 1991;7:295–307.
4. Takagi S, Kasuya Y, Shimizu M, Matsuura T, Tsuboi M, Kawakami A, et al. Expression of a cell adhesion molecule, neuropilin, in the developing chick nervous system. Dev Biol 1995;170:207–22.
5. He Z, Tessier-Lavigne M. Neuropilin is a receptor for the axonal chemorepellent Semaphorin III. Cell 1997;90:739–51.
6. Kolodkin AL, Levengood DV, Rowe EG, Tai YT, Giger RJ, Ginty DD. Neuropilin is a semaphorin III receptor. Cell 1997;90:753–62.
7. Chen H, Chedotal A, He Z, Goodman CS, Tessier-Lavigne M. Neuropilin-2, a novel member of the neuropilin family, is a high affinity receptor for the semaphorins Sema E and Sema IV but not Sema III. Neuron 1997;19:547–59.
8. Soker S, Takashima S, Miao HQ, Neufeld G, Klagsbrun M. Neuropilin-1 is expressed by endothelial and tumor cells as an isoform-specific receptor for vascular endothelial growth factor. Cell 1998;92:735–45.
9. Giger RJ, Urquhart ER, Gillespie SK, Levengood DV, Ginty DD, Kolodkin AL. Neuropilin-2 is a receptor for semaphorin IV: insight into the structural basis of receptor function and specificity. Neuron 1998;21:1079–92.
10. Gluzman-Poltorak Z, Cohen T, Herzog Y, Neufeld G. Neuropilin-2 is a receptor for the vascular endothelial growth factor (VEGF) forms VEGF-145 and VEGF-165 [corrected]. J Biol Chem 2000;275:18040–5.
11. Gammill LS, Gonzalez C, Gu C, Bronner-Fraser M. Guidance of trunk neural crest migration requires neuropilin 2/semaphorin 3F signaling. Development 2006;133:99–106.
12. Favier B, Alam A, Barron P, Bonnin J, Laboudie P, Fons P, et al. Neuropilin-2 interacts with VEGFR-2 and VEGFR-3 and promotes human endothelial cell survival and migration. Blood 2006;108:1243–50.
13. Kawasaki T, Kitsukawa T, Bekku Y, Matsuda Y, Sanbo M, Yagi T, et al. A requirement for neuropilin-1 in embryonic vessel formation. Development 1999;126:4895–902.
14. Giger RJ, Cloutier JF, Sahay A, Prinjha RK, Levengood DV, Moore SE, et al. Neuropilin-2 is required in vivo for selective axon guidance responses to secreted semaphorins. Neuron 2000;25:29–41.
15. Chen H, Bagri A, Zupicich JA, Zou Y, Stoeckli E, Pleasure SJ, et al. Neuropilin-2 regulates the development of selective cranial and sensory nerves and hippocampal mossy fiber projections. Neuron 2000;25:43–56.
16. Yuan L, Moyon D, Pardanaud L, Breant C, Karkkainen MJ, Alitalo K, et al. Abnormal lymphatic vessel development in neuropilin 2 mutant mice. Development 2002;129:4797–806.
17. Gray MJ, Van Buren G, Dallas NA, Xia L, Wang X, Yang AD, et al. Therapeutic targeting of neuropilin-2 on colorectal carcinoma cells implanted in the murine liver. J Natl Cancer Inst 2008;100:109–20.
18. Caunt M, Mak J, Liang WC, Stawicki S, Pan Q, Tong RK, et al. Blocking neuropilin-2 function inhibits tumor cell metastasis. Cancer Cell 2008;13:331–42.
19. Rushing EC, Stine MJ, Hahn SJ, Shea S, Eller MS, Naif A, et al. Neuropilin-2: a novel biomarker for malignant melanoma? Hum Pathol 2012;43:381–9.
20. Yasuoka H, Kodama R, Hirokawa M, Takamura Y, Miyauchi A, Inagaki M, et al. Neuropilin-2 expression in papillary thyroid carcinoma: correlation with VEGF-D expression, lymph node metastasis, and VEGF-D-induced aggressive cancer cell phenotype. J Clin Endocrinol Metab 2011;96:E1857–61.
21. Cohen T, Herzog Y, Brodzky A, Greenson JK, Eldar S, Gluzman-Poltorak Z, et al. Neuropilin-2 is a novel marker expressed in pancreatic islet cells and endocrine pancreatic tumours. J Pathol 2002;198:77–82.
22. Dallas NA, Gray MJ, Xia L, Fan F, van Buren G 2nd, Gaur P, et al. Neuropilin-2-mediated tumor growth and angiogenesis in pancreatic adenocarcinoma. Clin Cancer Res 2008;14:8052–60.
23. Handa A, Tokunaga T, Tsuchida T, Lee YH, Kijima H, Yamazaki H, et al. Neuropilin-2 expression affects the increased vascularization and is a prognostic factor in osteosarcoma. Int J Oncol 2000;17:291–5.
24. Yasuoka H, Kodama R, Tsujimoto M, Yoshidome K, Akamatsu H, Nakahara M, et al. Neuropilin-2 expression in breast cancer: correlation with lymph node metastasis, poor prognosis, and regulation of CXCR4 expression. BMC Cancer 2009;9:220.
25. Samuel S, Gaur P, Fan F, Xia L, Gray MJ, Dallas NA, et al. Neuropilin-2 mediated beta-catenin signaling and survival in human gastrointestinal cancer cell lines. PLoS One 2011;6:e23208.
26. Cao Y, Szabolcs A, Dutta SK, Yaqoob U, Jagavelu K, Wang L, et al. Neuropilin-1 mediates divergent R-Smad signaling and the myofibroblast phenotype. J Biol Chem 2010;285:31840–8.
27. Biankin AV, Waddell N, Kassahn KS, Gingras MC, Muthuswamy LB, Johns AL, et al. Pancreatic cancer genomes reveal aberrations in axon guidance pathway genes. Nature 2012;491:399–405.
28. Kent WJ. BLAT–the BLAST-like alignment tool. Genome Res 2002;12:656–64.
29. Barbosa-Morais NL, Dunning MJ, Samarajiwa SA, Darot JF, Ritchie ME, Lynch AG, et al. A re-annotation pipeline for Illumina BeadArrays: improving the interpretation of gene expression data. Nucleic Acids Res 2010;38:e17.
30. Puech PH, Taubenberger A, Ulrich F, Krieg M, Muller DJ, Heisenberg CP. Measuring cell adhesion forces of primary gastrulating cells from zebrafish using atomic force microscopy. J Cell Sci 2005;118:4199–206.
31. Friedrichs J, Helenius J, Muller DJ. Quantifying cellular adhesion to extracellular matrix components by single-cell force spectroscopy. Nat Protoc 2010;5:1353–61.

Published OnlineFirst May 20, 2013; DOI: 10.1158/0008-5472.CAN-13-0529




32. Helenius J, Heisenberg CP, Gaub HE, Muller DJ. Single-cell force spectroscopy. J Cell Sci 2008;121:1785–91.
33. Zhang X, Wojcikiewicz E, Moy VT. Force spectroscopy of the leukocyte function-associated antigen-1/intercellular adhesion molecule-1 interaction. Biophys J 2002;83:2270–9.
34. Zhang X, Chen A, De Leon D, Li H, Noiri E, Moy VT, et al. Atomic force microscopy measurement of leukocyte-endothelial interaction. Am J Physiol Heart Circ Physiol 2004;286:H359–67.
35. Hutter JL, Bechhoefer J. Calibration of atomic-force microscope tips. Rev Sci Instrum 1993;64:1868–73.
36. Cao Y, Wang L, Nandy D, Zhang Y, Basu A, Radisky D, et al. Neuropilin-1 upholds dedifferentiation and propagation phenotypes of renal cell carcinoma cells by activating Akt and sonic hedgehog axes. Cancer Res 2008;68:8667–72.
37. Motzer RJ, Bander NH, Nanus DM. Renal-cell carcinoma. N Engl J Med 1996;335:865–75.
38. Wallach JB, McGarry T, Torres J. Lymphangitic metastasis of recurrent renal cell carcinoma to the contralateral lung causing lymphangitic carcinomatosis and respiratory symptoms. Curr Oncol 2011;18:e35–7.
39. Stoletov K, Kato H, Zardouzian E, Kelber J, Yang J, Shattil S, et al. Visualizing extravasation dynamics of metastatic tumor cells. J Cell Sci 2010;123:2332–41.
40. Desgrosellier JS, Cheresh DA. Integrins in cancer: biological implications and therapeutic opportunities. Nat Rev Cancer 2010;10:9–22.
41. Jubb AM, Sa SM, Ratti N, Strickland LA, Schmidt M, Callahan CA, et al. Neuropilin-2 expression in cancer. Histopathology 2012;61:340–9.
42. Goel HL, Chang C, Pursell B, Leav I, Lyle S, Xi HS, et al. VEGF/neuropilin-2 regulation of Bmi-1 and consequent repression of IGF-IR define a novel mechanism of aggressive prostate cancer. Cancer Discov 2012;2:906–21.
43. Shimizu M, Murakami Y, Suto F, Fujisawa H. Determination of cell adhesion sites of neuropilin-1. J Cell Biol 2000;148:1283–93.
44. Murga M, Fernandez-Capetillo O, Tosato G. Neuropilin-1 regulates attachment in human endothelial cells independently of vascular endothelial growth factor receptor-2. Blood 2005;105:1992–9.
45. Valdembri D, Caswell PT, Anderson KI, Schwarz JP, Konig I, Astanina E, et al. Neuropilin-1/GIPC1 signaling regulates alpha5beta1 integrin traffic and function in endothelial cells. PLoS Biol 2009;7:e25.
46. Fukasawa M, Matsushita A, Korc M. Neuropilin-1 interacts with integrin beta1 and modulates pancreatic cancer cell growth, survival and invasion. Cancer Biol Ther 2007;6:1173–80.
47. Castellani V, Chedotal A, Schachner M, Faivre-Sarrailh C, Rougon G. Analysis of the L1-deficient mouse phenotype reveals cross-talk between Sema3A and L1 signaling pathways in axonal guidance. Neuron 2000;27:237–49.
48. Castellani V, De Angelis E, Kenwrick S, Rougon G. Cis and trans interactions of L1 with neuropilin-1 control axonal responses to semaphorin 3A. EMBO J 2002;21:6348–57.
49. Tordjman R, Ortega N, Coulombel L, Plouet J, Romeo PH, Lemarchandel V. Neuropilin-1 is expressed on bone marrow stromal cells: a novel interaction with hematopoietic cells? Blood 1999;94:2301–9.
50. Goel HL, Pursell B, Standley C, Fogarty K, Mercurio AM. Neuropilin-2 regulates alpha6beta1 integrin in the formation of focal adhesions and signaling. J Cell Sci 2012;125:497–506.
51. Antipenko A, Himanen JP, van Leyen K, Nardi-Dei V, Lesniak J, Barton WA, et al. Structure of the semaphorin-3A receptor binding module. Neuron 2003;39:589–98.
52. Love CA, Harlos K, Mavaddat N, Davis SJ, Stuart DI, Jones EY, et al. The ligand-binding face of the semaphorins revealed by the high-resolution crystal structure of SEMA4D. Nat Struct Biol 2003;10:843–8.
53. Valastyan S, Benaich N, Chang A, Reinhardt F, Weinberg RA. Concomitant suppression of three target genes can explain the impact of a microRNA on metastasis. Genes Dev 2009;23:2592–7.